sciendo

DOI 10.2478/ama-2025-0040

acta mechanica et automatica, vol.19 no.2 (2025)

ANALYSIS OF CONVECTIVE INSTABILITY IN DUSTY FERROMAGNETIC FLUIDS WITH MAGNETIC FIELD-DEPENDENT VISCOSITY UNDER FLUID-PERMEABLE MAGNETIC BOUNDARIES

Awneesh KUMAR*, Pankaj KUMAR*, Abhishek THAKUR*, Mandeep KAUR*

*Srinivasa Ramanujan Department of Mathematics, Central University of Himachal Pradesh, Kangra, Himachal Pradesh, India, 176206

ranaawneesh@gmail.com, pankajthakur28.85@hpcu.ac.in, abhishekthakur665@gmail.com, mandeepinspire2013@gmail.com

received 28 December 2024, revised 16 April 2025, accepted 03 May 2025

Abstract: The subject under consideration finds manifold applications across various disciplines, including biological, industrial, and environmental sectors. Therefore, this study aims to analytically investigate the onset of convective instability in a dusty ferromagnetic fluid layer, influenced by magnetic field-dependent viscosity and fluid-permeable magnetically active boundaries, when subjected to a uniform transverse magnetic field. The eigenvalue problem is formulated through the utilization of linear stability theory followed by normal mode analysis. To address this problem, a single-term Galerkin method is employed, followed by a numerical calculation of the critical magnetic Rayleigh number. It is investigated numerically and graphically that $(N_c)_{Free} \leq (N_c)_{Permeable} \leq (N_c)_{Rigid}$. It has been observed that as the dust particle parameter h_1 increase, the critical Rayleigh number decreases, indicating the destabilizing nature of h_1 On the other hand, the viscosity parameter δ and magnetic susceptibility χ and permeability parameter Da_s demonstrate a stabilizing effect on the system. Initially, measure of nonlinearity of magnetization M_3 exhibits a destabilizing effect, but beyond a certain threshold, it switches to a stabilizing effect within the system.

Key words: magnetic field-dependent viscosity, dust particles, ferrofluid, thermal convection, fluid-permeable magnetic boundaries

1. INTRODUCTION

Ferrofluids are unique types of fluids that exhibit both fluidic and magnetic properties. They are composed of stable colloidal suspensions of single-domain ferromagnetic or ferrimagnetic nanoparticles dispersed in a suitable liquid medium. The magnetic particles typically consist of ferromagnetic metals such as iron, nickel, and cobalt, or ferrimagnetic oxides like magnetite (Fe_3O_4) and spinel-type ferrites. Common carrier liquids include water, ethylene glycol, and various oils. The specific combination of magnetic particles and carrier fluid is chosen based on the intended application of the ferrofluid. Ferrofluids are widely used in sealing, damping, heat transfer, bearings, and sensors. They act as coolants in systems like loudspeakers and transformers, and enhance heat transfer in devices such as heat exchangers. Their use in exclusion seals helps protect sensitive components, making them valuable in robotics, textiles, electronics, and machinery [1, 2].

Due to their vast practical applications, researchers have conducted numerous experimental and theoretical studies on ferrofluids. These studies cover areas such as synthesis and characterization, heat transfer and thermal properties, theoretical modelling and simulation, and industrial applications [3, 4, 5]. Discussing the thermal stability of ferrofluids is equally important as examining their other properties. Understanding thermal stability ensures that ferrofluids can be effectively and safely utilized in current and future technologies.

Thermal stability of ferrofluid in the existence of a vertical magnetic field has been investigated by Finlayson [6]. Schwab et al. examined experimentally the Finlayson's problem [7]. Thermal stability of ferrofluid depends upon many factors such as density of ferrofluid, gravity acting on ferrofluid, medium of ferrofluid, Coriolis force on ferrofluid and hydrodynamic boundary conditions of ferrofluid. The influence of viscosity variation with magnetic field on thermal convection of ferrofluid has been explored by Sunil et al. [8]. whereas the viscosity variation with temperature field on thermal convection of ferrofluid for general boundary conditions has been investigated by Dhiman and Sharma [9, 10]. The porous medium plays a crucial role in directing geophysically detectable liquids into specific zones for imaging, controlled placement, or chemical treatment. Hence, analyzing the thermal stability of ferrofluids within a saturated porous layer is equally important. Vaidyanathan et al. [11] explored thermoconvective instability in a ferromagnetic fluid saturating a porous medium under the influence of a vertical magnetic field. Since rotation can significantly affect the thermal stability of a fluid layer, Venkatasubramanian and Kaloni [12] examined the impact of rotation on thermo-convective instability in a ferrofluid layer. Many authors have made remarkable contributions to exploring the impact of various parameters on ferrofluid convection (see references [13, 14, 15, 16, 17]).

There are many practical situations where ferrofluids may contain suspended particles. For instance, in industrial settings, ferrofluids are sometimes used as lubricants for machinery, particularly in high-precision equipment like bearings, seals, and pumps. However, in such environments, it is common for the ferrofluid to become contaminated with suspended particles. Therefore, studying ferrofluids with dust particles is equally important. Thermal stability of ferrofluid in the existence of dust particles is studied by Sunil et al. [18]. Sunil et al. [19] explored the impact of viscosity variation

with magnetic field on the thermal convection of dusty ferrofluids for the case of free-free boundaries. Sunil et al. [20] conducted a theoretical study on how magnetic field-dependent (MFD) viscosity influences thermal convection in a ferromagnetic fluid saturated porous medium containing dust particles. Sharma and Kumar [21] carried out a theoretical analysis of the combined influence of MFD viscosity and rotation on ferroconvection in a dusty fluid exposed to a uniform transverse magnetic field, whereas Kumar et al. [22] explored the impact of viscosity variation with temperature on the thermal convection of dusty ferrofluids of permeable boundaries. For a detailed understanding of thermal convection in dusty ferrofluids under various effects, one may refer to references [23, 24, 25, 26]. For further insights into related studies involving fluid systems containing dust particles and their significant effects, readers are referred to references [27, 28, 29, 30, 31].

The thermal stability of the liquid is determined by the thermal and hydrodynamic conditions at the surfaces that border it. In past works, fluid boundaries have been mainly either free-free or rigid-rigid. However, in many cases boundaries are neither purely free-free nor purely rigid-rigid. For instance, porous structures are used in cooling systems of electronic devices so as to facilitate ferrofluid movement and controlled heat transfer. Magnetic seals in rotating machinery consist of field-permeable membranes that maintain fluid position while allowing for fluid exchange and pressure fluctuations. For example, targeted drug delivery and hyperthermia treatment require ferrofluids to pass through semi-permeable biological membranes. Also heat exchangers, magnetic field-controlled filtration systems, ferrofluid-based microfluidic devices and aerospace thermal management all rely on boundary permeability for effective thermal convection. Siddheshwar [32] has documented the convective instability of ferromagnetic fluids confined by fluid-permeable and magnetically active boundaries. More recently, Nanjundappa et al. [26] explored penetrative ferro-thermal convection (FTC) driven by internal heating in a porous layer saturated with ferrofluid, considering various temperature, velocity, and magnetic potential boundary conditions. Additionally, Surya [33] examined convective instability of a liquid layer with permeable boundaries under the influence of variable gravitational force.

To the best of our knowledge, no prior studies have examined the combined effects of viscosity variation with magnetic fields and fluid-permeable magnetic boundary surfaces on the thermal convection of ferrofluids containing dust particles. This research is motivated by this gap in the literature. The study will provide different insights on how thermal convection can be optimized for various engineering applications such as electronics cooling, aerospace systems, biomedical technologies and environmental engineering through dust particles effects on it and variation of viscosity with magnetic field and fluid – permeable magnetic boundaries.

2. RESEARCH METHODOLOGY

The analytical investigation of convective instability in a dusty ferromagnetic fluid layer considering magnetic field-dependent viscosity and fluid-permeable, magnetically active boundaries under a uniform transverse magnetic field follows a structured approach aligned with the objectives of the study. A brief overview of the methodology is presented below as per the defined sections.

2.1. Fundamental Equations of the Problem

This phase includes recognizing and developing the core equations that govern the problem. These equations may be based on physical laws or derived from mathematical models.

2.2. Basic State

After establishing the fundamental equations, the system's basic state is identified. The system is considered to be in this basic state when there is no fluid motion in its initial condition.

2.3. Perturbation

Perturbations refer to small disturbances or deviations from the basic state that are introduced into the system. These disturbances enable the examination of the system's stability and behavior under different conditions [34].

2.4. Linear Analysis

To identify the instability threshold for an dusty ferromagnetic fluid during thermal convection, linear analysis specifically using normal mode analysis as described by Chandrasekhar [34] to create an eigenvalue problem offers valuable insights into the fundamental physics of thermal convection.

2.5. Normal Mode Analysis

Normal mode analysis is utilized to reduce the system of partial differential equations into an eigenvalue problem, which allows for a systematic examination of the stability of the system.

2.6. Non-dimensionalize the System of Equations

The governing equations of the system are non-dimensionalized to simplify the analysis and eliminate any reliance on specific units of measurement. Scaling factors are used to non-dimensionalize the perturbed equations.

2.7. Method of solution

The Galerkin method is employed to solve the eigenvalue problem, transforming it into a solvable system of algebraic equations. This method approximates the solution by selecting trial functions that satisfy the boundary conditions.

2.8. Result and discussion

Identify the effects of different parameters on the systems for different bounding surfaces, and interpret the results graphically.

3. MATHEMATICAL MODELLING

Consider a static layer of ferromagnetic fluid with a finite vertical thickness d and an infinite horizontal extent, heated from below, and containing dust particles. This fluid layer is subjected to a uniform vertical magnetic field $\boldsymbol{H}$ and experiences a gravitational force

represented by g and this system is confined between two horizontal fluid-permeable magnetic boundaries (as depicted in Fig. 1)

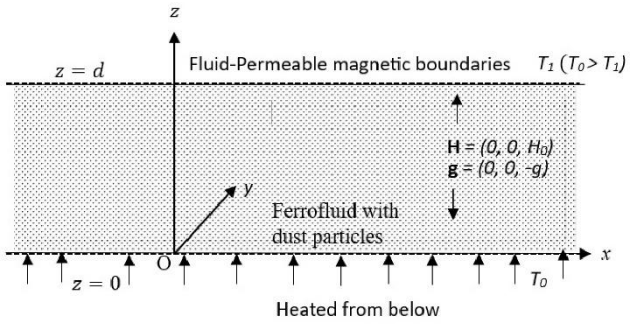

Fig. 1. Geometrical Configuration

We assume the fluid is incompressible, electrically non-conductive, and has a viscosity depend upon the magnetic field, expressed as $\mu = \mu_1(\delta.\boldsymbol{B} + 1)$ [35]. The fluid's viscosity when the magnetic field is zero is μ_1, the isotropic coefficient of viscosity change is δ, and the magnetic induction is represented by $\boldsymbol{B}$. For the model described, the governing equations under the Boussinesq approximation are provided by [6, 19]:

$$\nabla \cdot \boldsymbol{q} = 0\,, \tag{1}$$

$$\rho_0\left(\boldsymbol{q}\cdot\nabla + \frac{\partial}{\partial t}\right)\boldsymbol{q} - \rho g + \nabla p = \mu\nabla^2\boldsymbol{q} + \nabla\cdot(\boldsymbol{HB}) - KN_d(\boldsymbol{q}-\boldsymbol{q_d})\,, \tag{2}$$

$$mN_dC_{pt}\left(\frac{\partial}{\partial t} + \boldsymbol{q_d}\cdot\nabla\right)T - \left[\mu_0\boldsymbol{H}\cdot\left(\frac{\partial \boldsymbol{M}}{\partial T}\right)_{H,V} - \rho_0 C_{H,V}\right]\frac{DT}{Dt} + \mu_0 T\left(\frac{\partial \boldsymbol{M}}{\partial T}\right)_{H,V}\cdot\frac{D\boldsymbol{H}}{Dt} = K_1\nabla^2 T. \tag{3}$$

The equation of state for density is

$$\rho = \rho_0[1 + \alpha(T_0 - T)]\,, \tag{4}$$

In the aforementioned equations: $\boldsymbol{q}$ represents the ferrofluid's velocity, $\boldsymbol{q}_d$ indicates the dust particles' velocity, p pertains to pressure, ρ corresponds to density, N_d signifies the number density of the dust particles, M stands for magnetization, B represents magnetic induction, T is the temperature, $C_{H,V}$ characterizes the specific heat at constant magnetic field and volume, C_{pt} indicates the specific heat of dust particles, K_1 designates the thermal conductivity, α represents the coefficient of thermal expansion, and $K = 6\pi\mu r$ signifies the Stokes drag coefficient, where r represents the radius of the dust particle. Additionally, ρ_0 and μ_0 correspond to the density and magnetic permeability at the reference temperature.

The buoyant force acting on the dust particles is neglected [18, 23, 26]. It is further assumed that the spacing between the particles is much larger than their diameters, allowing inter-particle interactions to be disregarded. The influence of gravity, pressure, and viscous forces on the particles is assumed to be negligibly small and is thus omitted from consideration. An additional force term with this opposite direction must be included in the particles' equation of motion, because the force applied by the ferrofluid on the dust particles is equal in magnitude but opposite in direction to the force exerted by the dust particles on the ferrofluid. Let mN_d denote the mass of dust particles per unit volume; the motion and continuity equations for the dust particles, under these assumptions, are given as follows [19, 22]:

$$mN_d\left(\boldsymbol{q_d}\cdot\nabla + \frac{\partial}{\partial t}\right)\boldsymbol{q_d} = -N_dK(\boldsymbol{q_d} - \boldsymbol{q}), \tag{5}$$

$$\nabla\cdot(N_d\boldsymbol{q_d}) + \frac{\partial N_d}{\partial t} = 0. \tag{6}$$

Due to assumption that fluid is electrically non-conductive, the equations of Maxwell in the case where displacement current is absent for a non-conductive fluid can be stated as follows [6]:

$$\nabla\times\boldsymbol{H} = 0,\ \ \nabla\cdot\boldsymbol{B} = 0, \tag{7}$$

and

$$\boldsymbol{B} = \mu_0(\boldsymbol{M} + \boldsymbol{H}). \tag{8}$$

Thus, from equations (7) and (8), we get

$$\nabla\cdot(\boldsymbol{M} + \boldsymbol{H}) = 0. \tag{9}$$

The alignment of magnetization is governed by both the magnetic field's strength and temperature, resulting in the following relationship

$$\boldsymbol{M} = \left(\frac{\boldsymbol{H}}{H}\right)M(H,T), \tag{10}$$

and

$$M = M_0 + K_2(T_0 - T) - \chi(H_0 - H), \tag{11}$$

Where M_0 is the magnetization when temperature is T_0 and magnetic field is H_0, while

$$K_2 = -\left(\frac{\partial \boldsymbol{M}}{\partial T}\right)_{T_0,\ H_0},\ \chi = \left(\frac{\partial \boldsymbol{M}}{\partial H}\right)_{T_0,\ H_0}$$

represents the pyromagnetic coefficient and magnetic susceptibility respectively.

Equations (1) to (11) are solved for zero flow at base state and thus the basic state solutions are given by

$$\rho = \rho_b(z),\ p = p_{\{b\}(z)},\quad \boldsymbol{q_d} = (\boldsymbol{q_d})_b = \boldsymbol{0}\ ,\quad \boldsymbol{q} = \boldsymbol{q}_b = \boldsymbol{0},\ T = T_0 - \beta z = T_b(z),\quad \beta = \frac{T_0 - T_1}{d},\quad (N_d)_b = N_d = N_0,\ H_0 + M_0 = H_0^{ext},\quad \boldsymbol{H}_b = \left(H_0 - \frac{\beta K_2}{\chi+1}z\right)\widehat{\boldsymbol{k}},\quad \boldsymbol{M}_b = \left(M_0 + \frac{\beta K_2}{\chi+1}z\right)\widehat{\boldsymbol{k}}. \tag{12}$$

Further following Finlayson [6] perturbations are added to initial basic state as:

$$\rho = \rho_b(z) + \rho',\ p = p_b(z) + p',\ \boldsymbol{q_d} = (\boldsymbol{q_d})_b + \boldsymbol{q_d}',\ \boldsymbol{q} = \boldsymbol{q}_b + \boldsymbol{q}'\,,\ T = T_b(z) + \theta',\ N_d = (N_d)_b + N',\ \boldsymbol{M} = \boldsymbol{M}_b(z) + \boldsymbol{M}',\ \boldsymbol{H} = \boldsymbol{H}_b(z) + \boldsymbol{H}'. \tag{13}$$

Where the variables

$$\rho', p', \boldsymbol{q}' = (u', v', w'), \boldsymbol{q_d}' = (l', r', s'),\ \theta', \boldsymbol{M}' \text{ and } \boldsymbol{H}'$$

represent infinitesimal disturbances in density, pressure, velocity of ferrofluid, velocity of dust particles, magnetic field intensity, magnetization and temperature, respectively.

On introducing equation (13) into equations (1) to (11) and applying the basic state solutions, we derive the linearized perturbation equations in the form.

$$\frac{\partial u'}{\partial x} + \frac{\partial v'}{\partial y} + \frac{\partial w'}{\partial z} = 0, \tag{14}$$

$$[L_0\rho_0 + mN_0]\frac{\partial u'}{\partial t} = L_0\left[\mu_0(M_0 + H_0)\frac{\partial H_1'}{\partial z} + \mu_1[1 + \delta\mu_0(M_0 + H_0)]\nabla^2 u' - \frac{\partial p'}{\partial x}\right], \tag{15}$$

$$[L_0\rho_0 + mN_0]\frac{\partial v'}{\partial t} = L_0\left[\mu_0(\mathrm{M_0}+\mathrm{H_0})\frac{\partial \mathrm{H_2'}}{\partial \mathrm{z}} + \mu_1[1+\delta\mu_0(\mathrm{M_0}+\mathrm{H_0})]\nabla^2 \mathrm{v'} - \frac{\partial \mathrm{p'}}{\partial \mathrm{y}}\right], \quad (16)$$

$$[L_0\rho_0 + mN_0]\frac{\partial w'}{\partial t} = L_0\left[\mu_0(\mathrm{M_0}+\mathrm{H_0})\frac{\partial \mathrm{H_3'}}{\partial \mathrm{z}} + \mu_1[1+\delta\mu_0(\mathrm{M_0}+\mathrm{H_0})]\nabla^2 \mathrm{w'} - \frac{\partial \mathrm{p'}}{\partial \mathrm{z}} + \rho_0 g\alpha\theta' - \mu_0 K_2\beta H_3' + \frac{\mu_0 K_2^2\beta}{(\chi+1)}\theta'\right], \quad (17)$$

$$L_0\left[\left(\rho C_1 + N_0 m C_{pt}\right)\frac{\partial\theta'}{\partial t} - K_1\nabla^2\theta' - \mu_0 T_0 K_2\frac{\partial}{\partial t}\left(\frac{\partial\phi'}{\partial z}\right)\right] = L_0\left[\beta\left(\rho C_1 - \frac{\mu_0 T_0 K_2^2}{\chi+1}\right)w'\right] + N_0 m\beta C_{pt} w', \quad (18)$$

Here $\rho C_1 = \mu_0 H_0 K_2 + \rho_0 C_{H,V}$, $L_0 = \left(\frac{m}{K}\frac{\partial}{\partial t} + 1\right)$, also,

$$\frac{\partial}{\partial x}(M_1' + H_1') + \frac{\partial}{\partial y}(M_2' + H_2') + \frac{\partial}{\partial z}(M_3' + H_3') = 0, \quad \nabla\phi' = \boldsymbol{H}', \quad (19)$$

where ϕ' is the perturbed magnetic potential, and

$$M_3' + H_3' = H_3'(\chi+1) - K_2\,\theta', M_i' + H_i' = \left(1 + \frac{M_0}{H_0}\right)H_i'(i = 1,2).$$

Here we have considered that $\beta d K_2 << (\chi+1)H_0$. (Finlayson [6]).

Now, eliminating p', u', v' between equations (15) -(17) using equation (14), we get

$$[L_0\rho_0 + mN_0]\frac{\partial}{\partial t}(\nabla^2 w') - L_0\mu_1[1+\delta\mu_0(M_0 + H_0)]\nabla^4 w' = L_0\left(\rho_0 g\alpha + \frac{\mu_0 K_2^2\beta}{(\chi+1)}\right)(\nabla_1^2\theta') - L_0\mu_0 K_2\beta\nabla_1^2\frac{\partial\phi'}{\partial z}, \quad (21)$$

where

$$\nabla_1^2 = \frac{\partial^2}{\partial x^2} + \frac{\partial^2}{\partial y^2}, \nabla^2 = \nabla_1^2 + \frac{\partial^2}{\partial z^2}.$$

Also, from equations (19) and (20), we have

$$(\chi+1)\frac{\partial^2\phi'}{\partial z^2} + \left(\frac{M_0}{H_0} + 1\right)\nabla_1^2\phi' - \frac{\partial\theta'}{\partial z}K_2 = 0. \quad (22)$$

Now, following normal mode analysis assuming that all quantities characterizing the perturbation depend on $t, x, y,$ and z in the form

$$(w', \phi', \theta')(t, x, y, z) = e^{[nt+\iota(xk_{x1}+yk_{y1})]}[w^*(z), \phi^*(z), \theta^*(z)]. \quad (23)$$

In this context, we have wave numbers represented as k_{x1} and k_{y1} for the x and y directions, respectively. Additionally, n denotes the growth rate, and k is defined as the magnitude of the resultant wave number, calculated as the square root of the sum of the squares of k_{x1} and k_{y1} and using non dimensional parameters:

$$z_\star = \frac{z}{d}, D_\star = \frac{\partial}{\partial z_\star}, a = kd, \ \omega = \frac{nd^2}{\nu}, \ w_\star = \frac{d}{\nu}w^*, t_\star = \frac{\nu}{d^2}t, \theta_\star = \frac{K_1 a\sqrt{R}}{\rho C_1\beta d\nu}\theta^*, \phi_\star = \frac{(\chi+1)K_1 a\sqrt{R}}{k_2\rho C_1\beta\nu d^2}\phi^*, k_{1_\star} = \frac{k_1}{d^2}, \ \delta_\star = \delta\mu_0 H(\chi+1), \ \nu = \frac{\mu_1}{\rho_0}, \ P_r = \frac{\nu\rho C_1}{K_1}, \ \tau = \frac{m\nu}{Kd^2}, R = \frac{g\alpha\beta d^4\rho C_1}{K_1\nu},$$

$$M_1 = \frac{\mu_0 K_2^2\beta}{(\chi+1)\alpha\rho_0 g}, \ M_2 = \frac{\mu_0 T_0 K_2^2}{(\chi+1)\rho C_1}, \ M_3 = \frac{1+\frac{M_0}{H_0}}{(\chi+1)}, f = \frac{mN_0}{\rho_0}, L_{0_\star} = \left(\tau\frac{\partial}{\partial t_\star} + 1\right), h = \frac{mN_0 C_{pt}}{\rho C_1},$$

in equations (18), (21) and (22), we obtained the non-dimensional linearised equations as

$$(D^2 - a^2)[(\omega\tau+1)\{(M_3\delta+1)(D^2-a^2) - \omega\} - f\omega]w = (\omega\tau+1)[(M_1+1)\theta - M_1 D\phi]a\sqrt{R}, \quad (24)$$

$$(\omega\tau+1)\{P_r M_2\omega D\phi + (D^2 - a^2 - (1+h)\omega P_r)\theta\} = -[h + (\omega\tau+1)(1-M_2)]a\sqrt{R}w, \quad (25)$$

$$(D^2 - a^2 M_3)\phi = D\theta. \quad (26)$$

A real independent variable z in the range $0 \le z \le 1$ is used in the aforementioned equations. Here, the square of the wave number is represented by a^2, while differentiation with respect to z is shown by $D = \frac{d}{dz}$. The variables P_r, R, M_1, M_2 and M_3 correspond to the Prandtl number, Rayleigh number, magnetic number, a non-dimensional parameter, and measure of nonlinearity of the magnetization parameter, respectively. The parameters h and f are related to dust particles. The complex constant $\omega = \omega_r + \iota\omega_i$ signifies the complex growth rate, where ω_i and ω_r are real constants. The variables, $w(z) = w_i(z)\iota + w_r(z)$, $\phi(z) = \phi_i(z)\iota + \phi_r(z)$, and $\theta(z) = \theta_i(z)\iota + \theta_r(z)$, are all complex functions of the real variable z, while w_r, w_i, ϕ_r, ϕ_i, θ_r, θ_i, are the real components of these functions.

From a physical standpoint, equations (24) to (26) define an eigenvalue problem for R, which governs ferromagnetic convection within a ferrofluid layer containing dust particles. In these equations, w represents the vertical velocity, θ indicates the temperature, and ϕ denotes the amplitude of the magnetic potential. Since M_2 is of a very small magnitude (on the order of 10^{-6}) [6], its influence is negligible for further analysis, allowing equation (25) to be simplified as.

$$(\omega\tau+1)\left(D^2 - a^2 - \omega P_r(1+h)\right)\theta = -[1 + \omega\tau + h]a\sqrt{R}w. \quad (27)$$

For the scenario of stationary convection, setting $\omega = 0$ simplifies the eigenvalue problem into the following form:

$$(1+M_3\delta)(D^4 - 2a^2D^2 + a^4)w = [(M_1+1)\theta - M_1 D\phi]a\sqrt{R}, \quad (28)$$

$$(-a^2 + D^2)\theta = -[h+1]a\sqrt{R}w, \quad (29)$$

$$(D^2 - a^2 M_3)\phi = D\theta. \quad (30)$$

Since the ferrofluid layer is confined between two thermally conducting and fluid- permeable magnetic surfaces. Hence, we use the following fluid-permeable magnetic boundaries condition as proposed by ([6, 32, 36, 37]):

$-(Da_s)Dw + D^2w = w = 0$, at $z = 0$ and $(Da_s)Dw + D^2w = w = 0$, at $z = 1$,

$-a\phi + (1+\chi)D\phi$ at $z = 0$ and $a\phi + (1+\chi)D\phi$ at $z = 1$,

$\theta = 0$ at $z = 0$ and $z = 1$, (31)

where Da_s is the slip-D'Arcy number and χ is the magnetic susceptibility.

4. MATHEMATICAL ANALYSIS

The non-dimensionalized linear ODEs (28) to (30) along with boundary conditions (31) form the eigen value problem with R as Rayleigh number. To determine the Rayleigh number for the given boundary conditions (31), we will employ a single-term Galerkin method. Let's consider a single term in the expansions of w, θ, and ϕ as follows:

$$w = A_{11}w_1(z),\ \theta = B_{11}\,\theta_1(z), \phi =\ C_{11}\phi_1(z)\,, \qquad (32)$$

Here, A_{11}, B_{11}, and C_{11} are constants, and $w_1(z)$, $\theta_1(z)$, and $\phi_1(z)$ are appropriately selected trial functions that satisfy the necessary boundary conditions (31). By replacing w, θ, and ϕ with their respective expressions in equations (28) to (30), then multiplying each resulting equation by $w_1(z)$, $\theta_1(z)$, and $\phi_1(z)$ accordingly, and integrating by parts the necessary number of times while applying the boundary conditions, we derive three homogeneous equations in A_{11}, B_{11}, and C_{11} . The coefficients of these equations are expressed as definite integrals. This system can be expressed in matrix form as follows:

$$\begin{pmatrix} (M_3\delta+1)A_2 & -a\sqrt{R}(1+M_1)A_3 & a\sqrt{R}M_1A_5 \\ (1+h_1)a\sqrt{R}A_3 & -A_1 & 0 \\ 0 & A_4 & A_6 \end{pmatrix}\begin{pmatrix} A_{11} \\ B_{11} \\ C_{11} \end{pmatrix} = \begin{pmatrix} 0 \\ 0 \\ 0 \end{pmatrix}$$

were,

$$A_1 = \int_0^1[(D\theta)^2 + a^2\theta^2]\ dz,$$

$$A_2 = \int_0^1[(D^2w)^2 + 2a^2(Dw)^2 + a^4(w)^2]\ dz + (Da_s)\left[\left(Dw(0)\right)^2 + \left(Dw(1)\right)^2\right],$$

$$A_3 = \int_0^1 w\,\theta\ dz,$$

$$A_4 = \int_0^1 \phi D\theta\ dz,$$

$$A_5 = \int_0^1 wD\phi\ dz,$$

$$A_6 = \int_0^1[(D\phi)^2 + a^2M_3\phi^2]\ dz + \frac{a}{\chi+1}[\phi(0)^2 + \phi(1)^2].$$

For simplicity, the subscript 1 is omitted, and the functions $w_1(z)$, $\theta_1(z)$, and $\phi_1(z)$ are henceforth denoted as w, θ, and ϕ respectively.

For a non-trivial solution to occur, the determinant of the coefficient matrix must be zero. This results in the following expression, which establishes a first-order relationship between the Rayleigh number R and the wave number a.

$$R = \frac{(M_3\delta+1)A_1A_2}{a^2(1+h)A_3\left\{(M_1+1)A_3+\frac{M_1A_4A_5}{A_6}\right\}}. \qquad (33)$$

Let us now select the following trial functions that satisfy the specified boundary conditions.

$$w = \frac{2}{2+Da_s}z + \frac{Da_s}{2+Da_s}z^2 - 2z^3 + z^4, \theta = z - z^2, \phi = -\frac{1}{2} + z. \qquad (34)$$

The initially proposed trial function for the magnetic potential, denoted by ϕ, does not meet the boundary conditions given in equation (31). To resolve this inconsistency, the boundary residual method, as described by Finlayson [6], is applied to the function ϕ.

By applying these trial functions to the integrals A_1 through A_6, we derive the following formula for Rayleigh number as

$$R = \frac{5880(M_3\delta+1)(x+10)\left[\frac{6\sqrt{x}}{1+\chi}+12+xM_3\right]\left[\left(\frac{4}{5}+4P\right)+\left(\frac{P^2}{30}+\frac{P}{70}+\frac{1}{630}\right)x^2+2\left(\frac{P^2}{3}+\frac{2P}{15}+\frac{2}{105}\right)x\right]}{h_1x(3+14P)\left\{(M_1+1)(3+14P)\left(\frac{6\sqrt{x}}{1+\chi}+12+xM_3\right)-28(1+5P)M_1\right\}} \qquad (35)$$

where $P = \frac{2}{2+Da_s}$, $h_1 = h + 1$ and $x = a^2$.

Using MATLAB R2023a software, the square of the critical wave number x_c is determined by finding the positive roots of the equation $\frac{dR}{dx} = 0$. Additionally, the associated critical Rayleigh number R_c is numerically calculated.

Also, we have the following formula for the magnetic Rayleigh number N for significantly large values of M_1 derived from expression (35) utilizing Finlayson [6] analysis.

$$N = \frac{5880(M_3\delta+1)(x+10)\left[\frac{6\sqrt{x}}{1+\chi}+12+xM_3\right]\left[\left(\frac{4}{5}+4P\right)+\left(\frac{P^2}{30}+\frac{P}{70}+\frac{1}{630}\right)x^2+2\left(\frac{P^2}{3}+\frac{2P}{15}+\frac{2}{105}\right)x\right]}{h_1x(3+14P)\left\{(M_1+1)(3+14P)\left(\frac{6\sqrt{x}}{1+\chi}+12+xM_3\right)-28(1+5P)M_1\right\}} \qquad (36)$$

which stand for the magnetic mechanism that functions when buoyancy effects are not present.

5. RESULTS AND DISCUSSION

This study explores the convective instability of a dusty ferromagnetic fluid, incorporating the effects of viscosity that depend on the magnetic field. The system is analyzed within a Rayleigh-Bènard configuration, where the fluid is contained between permeable boundaries that are also magnetically active. Additionally,the setup is subject to a uniform transverse magnetic field. Given the complexity of the boundary conditions, the Galerkin method was employed to calculate the critical eigenvalue. These findings can contribute to better control of instability in engineering systems and enhance the efficiency of applications where stability and precise thermal regulation are essential.

In the present analysis, the nonlinearity of the magnetization parameter M_3 is considered to vary from 0 to 25, as suggested by Finlayson [6]. The MFD viscosity parameter δ ranges from 0 to 0.09, as per the work of Prakash et al. [14]. The dust particle parameter h_1 is taken to vary between 1 and 9, following the suggestion of Sunil et al. [18]. Furthermore, the magnetic susceptibility of boundaries χ and the permeability parameter of boundaries Da_s are assumed to range from 10^0 to 10^6 and from 0 to ∞, respectively, as suggested by Siddheshwar [32].

First, we discuss the accuracy of the results presented in this study. For the case of ordinary fluid, in the absence of a magnetic parameter ($M_1 = 0$ and $M_3 = 0$), $\chi \to \infty$ and without dust particles ($h_1 = 1$), the critical Rayleigh number (R_c) and wave number (a_c^2) are found to be $R_c = 664.5251$ at $a_c^2 = 4.9594$ for free boundaries. This closely matches to $R_c = 657.551$ at $a_c^2 = 4.9328$ as obtained by Surya [33]. Additionally, for rigid boundaries, we have $R_c = 1750.0$ at $a_c^2 = 9.7127$, which closely matches $R_c = 1715.070$ at $a_c^2 = 9.6969$, as reported by Surya [33].

Also, Tab. 1 provide a qualitative comparison of the numerical results computed at $\chi \to \infty$, without dust particle ($h_1 = 1$), $M_3 = 10$, $M_1 = 1{,}5$ for the case of free-free and rigid-rigid boundaries

with Dhiman [10]. The table clearly shows that our results align exceptionally well with previously published data, confirming the accuracy of our numerical procedure.

Tab. 1. Comparison of Values from the Present Study with Existing Studies

	Free-Free		Rigid-Rigid	
	Present Study	Dhiman [10]	Present Study	Dhiman [10]
	$R_c(a_c^2)$	$R_c(a_c^2)$	$R_c(a_c^2)$	$R_c(a_c^2)$
$M_1 = 1$	360.0088 (5.4644)	342.52 (5.174)	913.1268 (10.2291)	889.15 (9.921)
$M_1 = 5$	126.5677 (5.8260)	116.49 (5.319)	313.1211 (10.5816)	299.56 (10.06)

Tab. 2. Variation of critical magnetic Rayleigh numbers N_c with M_3 , χ and δ at fixed $h_1 = 3$ and $Da_s = 1$

$h_1 = 3$		Critical Magnetic Rayleigh Number $N_c(a_c^2)$ at				
χ	M_3	$\delta = 0.01$	$\delta = 0.03$	$\delta = 0.05$	$\delta = 0.07$	$\delta = 0.09$
1	1	412.4400 (7.7909)	420.6071 (7.7909)	428.7742 (7.7909)	436.9413 (7.7909)	445.1085 (7.7909)
	5	333.0876 (7.0576)	364.8102 (7.0576)	396.5328 (7.0576)	428.2554 (7.0576)	459.9781 (7.0576)
	10	321.2218 (6.6092)	379.6257 (6.6092)	438.0297 (6.6092)	496.4336 (6.6092)	554.8376 (6.6092)
	15	323.9978 (6.3847)	408.5190 (6.3847)	493.0402 (6.3847)	577.5614 (6.3847)	662.0825 (6.3847)
	20	331.3287 (6.2498)	441.7716 (6.2498)	552.2144 (6.2498)	662.6573 (6.2498)	773.1002 (6.2498)
10	1	494.4820 (8.9375)	504.2737 (8.9375)	514.0654 (8.9375)	523.8572 (8.9375)	533.6489 (8.9375)
	5	342.8150 (7.3292)	375.4640 (7.3292)	408.1130 (7.3292)	440.7621 (7.3292)	473.4111 (7.3292)
	10	324.5245 (6.7147)	383.5290 (6.7147)	442.5334 (6.7147)	501.5379 (6.7147)	560.5423 (6.7147)
	15	325.7133 (6.4415)	410.6820 (6.4415)	495.6507 (6.4415)	580.6194 (6.4415)	665.5881 (6.4415)
	20	332.4015 (6.2855)	443.2020 (6.2855)	554.0025 (6.2855)	664.8030 (6.2855)	775.6035 (6.2855)
10^3	1	525.1702 (9.3988)	535.5696 (9.3988)	545.9690 (9.3988)	556.3685 (9.3988)	566.7679 (9.3988)
	5	345.3312 (7.4019)	378.2199 (7.4019)	411.1086 (7.4019)	443.9972 (7.4019)	476.8859 (7.4019)
	10	325.3216 (6.7407)	384.4710 (6.7407)	443.6204 (6.7407)	502.7697 (6.7407)	561.9191 (6.7407)
	15	326.1164 (6.4551)	411.1902 (6.4551)	496.2641 (6.4551)	581.3379 (6.4551)	666.4118 (6.4551)
	20	332.6499 (6.2938)	443.5332 (6.2938)	554.4166 (6.2938)	665.2999 (6.2938)	776.1832 (6.2938)
10^5	1	525.5497 (9.4046)	535.9567 (9.4046)	546.3636 (9.4046)	556.7705 (9.4046)	567.1774 (9.4046)
	5	345.3597 (7.4027)	378.2512 (7.4027)	411.1426 (7.4027)	444.0340 (7.4027)	476.9254 (7.4027)
	10	325.3305 (6.7410)	384.4815 (6.7410)	443.6325 (6.7410)	502.7835 (6.7410)	561.9345 (6.7410)
	15	326.1209 (6.4552)	411.1959 (6.4552)	496.2709 (6.4552)	581.3459 (6.4552)	666.4209 (6.4552)
	20	332.6527 (6.2939)	443.5369 (6.2939)	554.4212 (6.2939)	665.3054 (6.2939)	776.1896 (6.2939)

Tab. 2 presented the numerical values of critical magnetic Rayleigh number (N_c) and square of critical wave number (a_c^2) for different combination of δ, M_3, χ at fixed h_1=3 and $Da_s = 1$. Tab. 4 presented the numerical values of critical magnetic Rayleigh number (N_c) and square of critical wave number (a_c^2) for different combination of h_1, Da_s and M_3 at fixed δ=0.03 and $\chi = 10$.

Fig. 2 depict the variation of critical magnetic Rayleigh numbers N_c versus χ with different values of M_3 and fixed values of δ, h_1 and Da_s. From Fig. 2 and numerical values of critical magnetic Rayleigh numbers N_c presented in Tab. 3 we can observe that critical magnetic Rayleigh numbers increases for increasing values of χ, which yields that χ has stabilizing effect on the system. This stabilizing effect of χ directly depend upon M_3, χ has strong stabilizing effect for smaller values of M_3 as compare to larger values of M_3 . Also from Tab.3 we can observe that the critical wave number increases as χ increases which indicate that χ reduces the size of convection cell.

Fig.3 depict the variation of critical magnetic Rayleigh numbers N_c versus Da_s with different values of δ and fixed values of M_3, h_1 and χ. From Fig. 3 and numerical values of critical magnetic Rayleigh numbers N_c presented in Tab. 4 we can observe that critical magnetic Rayleigh numbers increases for increasing values of Da_s, which yields that Da_s has stabilizing effect on the system. Also we can conclude that $(N_c)_{\boldsymbol{Free}} \leq (N_c)_{\boldsymbol{Permeable}} \leq (N_c)_{\boldsymbol{Rigid}}$. Because $(N_c)_{\boldsymbol{Free}}$ and $(N_c)_{\boldsymbol{Rigid}}$ can be acquired from $(N_c)_{\boldsymbol{Permeable}}$ in the limit $Da_s \to 0$ and ∞ respectively. Therefore the equality sign in $(N_c)_{\boldsymbol{Free}} \leq (N_c)_{\boldsymbol{Permeable}} \leq (N_c)_{\boldsymbol{Rigid}}$ is understandable. This analysis effectively demonstrates the connection between the results for free-free and rigid-rigid boundary conditions. This behavior arises because free boundaries impose minimal resistance to fluid motion near the surfaces, allowing the temperature gradient to drive convection more easily. As a result, the fluid becomes more responsive to instabilities, leading to a lower critical magnetic Rayleigh number and an earlier onset of convection compared to the case with rigid boundaries. Further, it is evident from Tab.4 that the critical wave number increases as Da_sincreases which indicate that Da_s reduces the size of convection cell.

Fig. 4 depict the variation of critical magnetic Rayleigh numbers N_c versus δ with different values of M_3 and fixed values of χ, h_1

DOI 10.2478/ama-2025-0040

and Da_s. From Fig. 3, Fig. 4, Fig. 5, Fig.7 and numerical values of critical magnetic Rayleigh numbers N_c presented in Tab.3 we can observe that critical magnetic Rayleigh numbers increases for increasing values of δ, which yields that δ has stabilizing effect on the system. This is consistent with the physical understanding that higher viscosity suppresses disturbances and restricts fluid movement, resulting in a delayed onset of convection. Also, it is noted from table Tab.3 that the critical wave number has no influence of MFD viscosity δ, i.e. size of convection cell is independent of MFD viscosity δ.

Tab. 3. Variation of critical magnetic Rayleigh numbers N_c with h_1, M_3 and Da_s at fixed $\chi = 10$ and $\delta = 0.03$

$\chi = 10$		Critical Magnetic Rayleigh Number $N_c(a_c^2)$ at				
M_3	h_1	$Da_s = 0$	$Da_s = 10$	$Da_s = 10^2$	$Da_s = 10^3$	$Da_s = 10^5$
3	1	1058.2 (7.1019)	1713.5 (10.3132)	2257.1 (11.8650)	2371.8 (12.1002)	2385.8 (12.1272)
	3	352.7195 (7.1019)	571.1730 (10.3132)	752.3706 (11.8650)	790.5888 (12.1002)	795.2814 (12.1272)
	5	211.6317 (7.1019)	342.7038 (10.3132)	451.4224 (11.8650)	474.3533 (12.1002)	477.1689 (12.1272)
	7	151.1655 (7.1019)	244.7884 (10.3132)	322.4445 (11.8650)	338.8238 (12.1002)	340.8349 (12.1272)
	9	117.5732 (7.1019)	190.3910 (10.3132)	250.7902 (11.8650)	263.5296 (12.1002)	265.0938 (12.1272)
5	1	998.5998 (6.5835)	1660.7 (9.6886)	2210.0 (11.1916)	2325.7 (11.4193)	2339.9 (11.4454)
	3	332.8666 (6.5835)	553.5690 (9.6886)	736.6527 (11.1916)	775.2371 (11.4193)	779.9737 (11.4454)
	5	199.7200 (6.5835)	332.1414 (9.6886)	441.9916 (11.1916)	465.1422 (11.4193)	467.9842 (11.4454)
	7	142.6571 (6.5835)	237.2439 (9.6886)	315.7083 (11.1916)	332.2445 (11.4193)	334.2744 (11.4454)
	9	110.9555 (6.5835)	184.5230 (9.6886)	245.5509 (11.1916)	258.4124 (11.4193)	259.9912 (11.4454)
10	1	1010.8 (5.9857)	1734.0 (9.0216)	2332.5 (10.4899)	2458.4 (10.7120)	2473.8 (10.7375)
	3	336.9392 (5.9857)	578.0082 (9.0216)	777.4880 (10.4899)	819.4643 (10.7120)	824.6157 (10.7375)
	5	202.1635 (5.9857)	346.8049 (9.0216)	466.4928 (10.4899)	491.6786 (10.7120)	494.7694 (10.7375)
	7	144.4025 (5.9857)	247.7178 (9.0216)	333.2092 (10.4899)	351.1990 (10.7120)	353.4067 (10.7375)
	9	112.3131 (5.9857)	192.6694 (9.0216)	259.1627 (10.4899)	273.1548 (10.7120)	274.8719 (10.7375)
15	1	1077.7 (5.7151)	1875.3 (8.7376)	2534.0 (10.1969)	2672.5 (10.4175)	2689.5 (10.4428)
	3	359.2290 (5.7151)	625.0951 (8.7376)	844.6717 (10.1969)	890.8388 (10.4175)	896.5038 (10.4428)
	5	215.5374 (5.7151)	375.0570 (8.7376)	506.8030 (10.1969)	534.5033 (10.4175)	537.9023 (10.4428)
	7	153.9553 (5.7151)	267.8979 (8.7376)	362.0022 (10.1969)	381.7881 (10.4175)	384.2159 (10.4428)
	9	119.7430 (5.7151)	208.3650 (8.7376)	281.5572 (10.1969)	296.9463 (10.4175)	298.8346 (10.4428)

The behavior of the critical magnetic Rayleigh number N_c as a function of M_3 is illustrated in Fig. 6 for several values of χ, while keeping M_3, h_1 and δ constant. Similarly, Fig. 7 depicts the relationship between N_c and M_3 for different values of δ, with h_1, M_3, and χ held fixed. The critical magnetic Rayleigh number N_c initially decreases for increasing values of M_3, but after a certain value of M_3, it increases for increasing values of M_3, as shown by Fig. 2, Fig. 4, Fig. 6, Fig. 7 and Tab. 2 as well as Tab. 3. This destabilizing or stabilizing effect of M_3 varies upon the value of δ. The destabilizing effect range of M_3 is larger for small values of δ than it is at large values of δ. From Tab. 2 and Tab. 3 it is observed that critical wave number reduces with raise in M_3 which means that M_3 increases the size of convection cell.

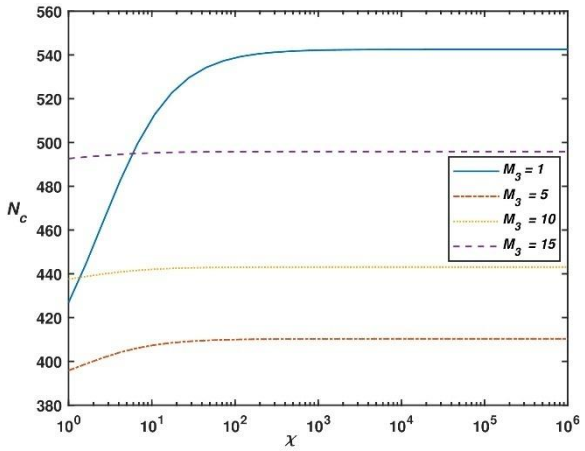

Fig. 2. Graph between $N_c$vs χ at $\delta = 0.05$, $h_1 = 3$ and $Da_s = 1$

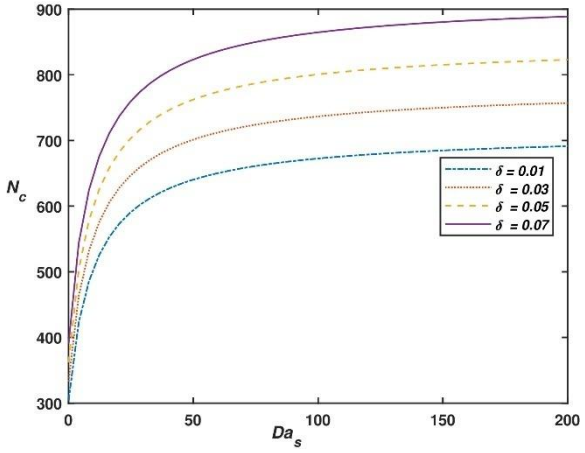

Fig. 3. Graph between N_c vs Da_s at h_1=3, $\chi = 10$ and $M_3 = 5$

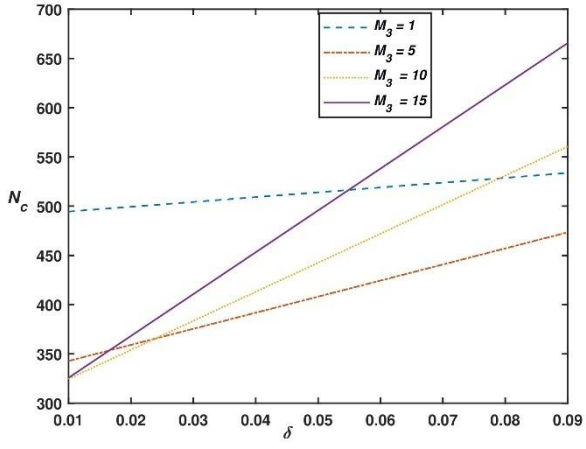

Fig. 4. Graph between N_c vs δ at $\chi = 10$, $Da_s = 1$ and $h_1 = 3$

The behavior of the critical magnetic Rayleigh number N_c as a function of dust particles parameter h_1 is illustrated in Fig. 5 for

several values of δ, while keeping h_1, M_3, and χ constant. From Fig. 2 and numerical values of critical magnetic Rayleigh numbers N_c presented in table Tab. 2 we can observe that critical magnetic Rayleigh numbers decreases for increasing values of h_1, which shows that h_1 has destabilizing effect on the system as the overall heat capacity of the fluid increases due to the additional contribution from the dust particles. Moreover Tab. 2 demonstrates that the critical wave number does not depend on the parameter h_1 of dust particles, meaning that the size of the convection cell is not affected by dust particles parameter h_1.

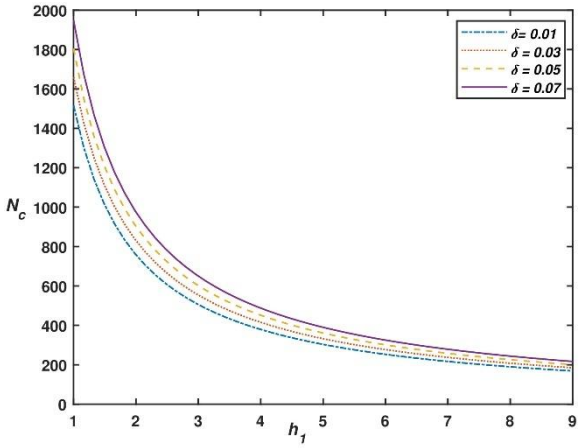

Fig. 5. Graph between N_c vs h_1 at $Da_s = 10$, $\chi = 10$ and $M_3 = 5$

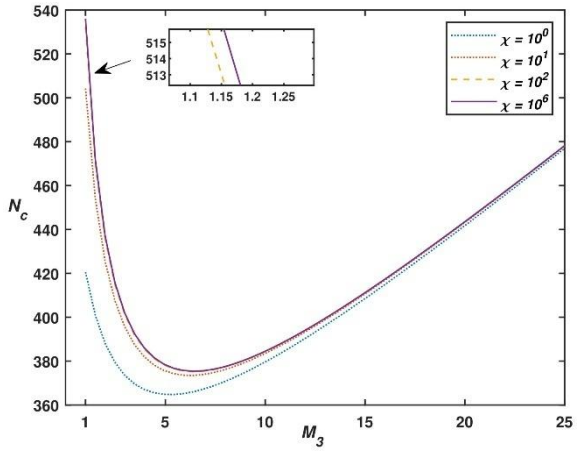

Fig. 6. Graph between N_c vs M_3 at $\delta = 0.03$, $Da_s = 1$ and $h_1 = 3$

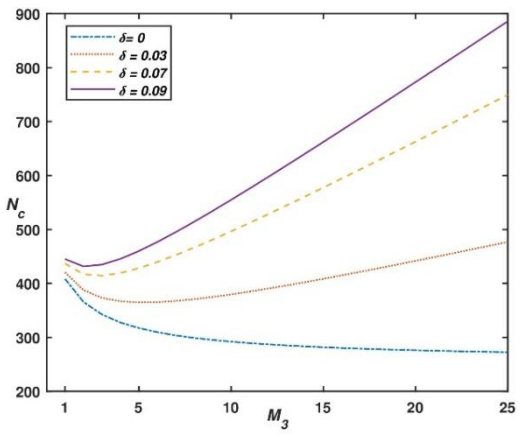

Fig. 7. Graph between N_c vs M_3 at $\chi = 1$, $Da_s = 1$ and $h_1 = 3$

6. CONCLUSION

For a Rayleigh-Bénard situation between fluid-permeable, magnetic boundaries, we investigate the impact of dust particles and viscosity variation with magnetic field on the convective instability of a ferro magnetic fluid layer using the single term Galerkin technique for stationary mode of convection. The main conclusion from our research can be summarized as follows:

- The parameters of fluid permeable, magnetic boundaries and MFD viscosity parameter delay the initiation of onset of convection which indicate their stabilizing effect.
- Dust particles parameter h_1 initiate the initiation of onset of convection which indicate their destabilizing effect.
- Measure of nonlinearity of magnetization M_3 exhibits a destabilizing effect, but beyond a certain threshold, it switches to a stabilizing effect within the system.
- The size of cells formed at the initiation of convection narrows with a raise in the parameter of permeable magnetic boundaries.
- The size of cells formed at the initiation of convection widens with a raise in the measure of nonlinearity of magnetization M_3.
- The dust particles parameter and MFD viscosity has no effect on the size of cell formed at the initiation of convection.

These discoveries advance our knowledge of the variables affecting convection of ferrofluid and offer useful data for a number of disciplines, including fluid dynamics and geophysics. Additional investigation in this field may clarify our understanding of convection phenomena and examine the practical consequences of these results.

Nomenclature

Symbol	Explanation
d	Depth of the ferromagnetic fluid layer (m)
t	Time variable (s)
T	Temperature (K)
T_0, T_1	Reference temperatures at $z = 0$ and $z = d$ respectively (K)
r	Radius of a dust particle (m)
m	Mass of a dust particle (kg)
N_d	Number density of dust particles (particles/m^3)
N'	Disturbance to number density of dust particles (particles/m^3)
C_{pt}	Heat capacity of dust particles (kJ/m^3K)
$C_{H,V}$	Specific heat at constant magnetic field and volume (kJ/m^3K)
K_1	Thermal conductivity $(\frac{W}{mK})$
K_2	Pyromagnetic coefficient = $-\partial M/\partial T$ at (T_0, H_0) (A/mK)
K	Stokes drag coefficient (kg/s)
Da_s	Darcy number accounting for velocity slip
p	Fluid pressure (psi)
p'	Pressure perturbation (psi)
$\boldsymbol{q}$	Velocity of the ferrofluid (m/s)
$\boldsymbol{q}' = (u', v', w')$	Velocity perturbation of the fluid (m/s)
$\boldsymbol{q_d}$	Dust particle velocity (m/s)
$\boldsymbol{q_d}' = (l', r', s')$,	Dust velocity disturbance (m/s)

g	Gravitational acceleration, $g = (0, 0, -g)\ (m/s^2)$
D/Dt	Convective (material) derivative (s^{-1})
k_{x1}, k_{y1}	Horizontal wave numbers in x and y directions (m^{-1})
k	Overall wave number, $k = \sqrt{({k_{x1}}^2 + {k_{y1}}^2)}\ (m^{-1})$
$\widehat{\boldsymbol{k}}$	Unit vector in the vertical (z) direction
$\boldsymbol{H}$	Magnetic field vector (A/m)
H, H^0, H^{ext}	Magnitude of field, reference field, and external magnetic field (A/m)
$\boldsymbol{H'}$	Magnetic field perturbation (A/m)
$\boldsymbol{B}$	Magnetic flux density (T)
B	Magnitude of magnetic induction (T)
$\boldsymbol{M}$	Magnetization (A/m)
$\boldsymbol{M'}$	Magnetization disturbance (A/m)
M_0	Magnetization at $(H_0, T_0)\ (A/m)$
b	Subscript indicating base (equilibrium) state
Greek Symbols	
α	Thermal expansion coefficient (K^{-1})
β	Constant thermal gradient $\lvert dT/dz \rvert\ (K/m)$
ν	Kinematic viscosity (m^2/s)
μ	Dynamic viscosity $(kg/m \cdot s)$
μ_1	Dynamic viscosity under ambient magnetic field $(kg/m \cdot s)$
μ_0	Magnetic permeability of vacuum (H/m)
ρ	Fluid density (kg/m^3)
ρ_0	Reference density at $T_0\ (kg/m^3)$
ρ'	Density perturbation (kg/m^3)
θ'	Temperature fluctuation (K)
ω	Rate of growth of disturbances (s^{-1})
χ	Magnetic susceptibility $= \partial M/\partial H$ at (T_0, H_0)
∇	Gradient (del) operator (m^{-1})
ϕ'	Perturbation in magnetic scalar potential (A)

REFERENCES

1. Scherer C, Figueiredo Neto AM. Ferrofluids: properties and applications. Braz J Phys. 2005;35(3A):718–727. https://doi.org/10.1590/S0103-97332005000400018
2. Kole M, Khandekar S. Engineering applications of ferrofluids: A review. J Magn Magn Mater. 2021;537:168222. https://doi.org/10.1016/j.jmmm.2021.168222
3. Genc S, Derin B. Synthesis and rheology of ferrofluids: a review. Curr Opin Chem Eng. 2014;3:118–124. https://doi.org/10.1016/j.coche.2013.12.006
4. Alsaady M, Fu R, Li B, Boukhanouf R, Yan Y. Thermo-physical properties and thermo-magnetic convection of ferrofluid. Appl Therm Eng. 2015;88:14–21. https://doi.org/10.1016/j.applthermaleng.2014.09.087
5. Ivanov AO, Kantorovich SS, Reznikov EN, Holm C, Pshenichnikov AF, Lebedev AV, et al. Magnetic properties of polydisperse ferrofluids: A critical comparison between experiment, theory, and computer simulation. Phys Rev E. 2007;75(6):061405. https://doi.org/10.1103/PhysRevE.75.061405
6. Finlayson BA. Convective instability of ferromagnetic fluids. J Fluid Mech. 1970;40(4):753–767. https://doi.org/10.1017/S0022112070000423
7. Schwab L, Hildebrandt U, Stierstadt K. Magnetic Bénard convection. J Magn Magn Mater. 1983;39(1–2):113–114. https://doi.org/10.1016/0304-8853(83)90412-2
8. Sunil, Sharma A, Sharma D, Kumar P. Effect of magnetic field–dependent viscosity on thermal convection in a ferromagnetic fluid. Chem Eng Commun. 2008;195(5):571–583. https://doi.org/10.1080/00986440701707719
9. Dhiman J, Sharma N. Thermal instability of hot ferrofluid layer with temperature-dependent viscosity. Int J Fluid Mech Res. 2018;45(5):389–398. https://doi.org/10.1615/InterJFluidMechRes.2018016842
10. Dhiman JS, Sharma N. Effect of temperature dependent viscosity on thermal convection in ferrofluid layer. J Theor Appl Mech. 2021; 51:3–21.
11. Vaidyanathan G, Sekar R, Balasubramanian R. Ferroconvective instability of fluids saturating a porous medium. Int J Eng Sci. 1991;29(10):1259–1267. https://doi.org/10.1016/0020-7225(91)90029-3
12. Venkatasubramanian S, Kaloni PN. Effects of rotation on the thermoconvective instability of a horizontal layer of ferrofluids. Int J Eng Sci. 1994;32(2):237–256. https://doi.org/10.1016/0020-7225(94)90004-3
13. Chand P, Bharti PK, Mahajan A, et al. Thermal convection in micropolar ferrofluid in the presence of rotation. J Magn Magn Mater. 2008;320(3–4):316–324. https://doi.org/10.1016/j.jmmm.2007.06.006
14. Prakash J, Manan S, Kumar P. Ferromagnetic convection in a sparsely distributed porous medium with magnetic field dependent viscosity revisited. J Porous Media. 2018;21(8). https://doi.org/10.1615/JPorMedia.2018018832
15. Prakash J, Kumar P, Manan S, Sharma K. The effect of magnetic field dependent viscosity on ferromagnetic convection in a rotating sparsely distributed porous medium-revisited. Int J Appl Mech Eng. 2020;25(1):142–158. https://doi.org/10.2478/ijame-2020-0010
16. Kumar P, Kaur M, Thakur A, Bala R. On estimating the growth rate of perturbations in Rivlin-Ericksen ferromagnetic convection with magnetic field dependent viscosity. Tech Mech. 2024;44(1):1–13. https://doi.org/10.24352/UB.OVGU-2024-0512024
17. Kaur M, Kumar P, Manan S, Kumar A. Combined effect of magnetic field dependent viscosity and fluid-permeable, magnetic boundaries on convective instabilities in a hot ferrofluid layer. J Taibah Univ Sci. 2025;19(1):2464462. https://doi.org/10.1080/16583655.2025.2464462
18. Sunil, Sharma A, Sharma D, Sharma R. Effect of dust particles on thermal convection in a ferromagnetic fluid. Z Naturforsch A. 2005;60(7):494–502. https://doi.org /10.1515/zna-2005-0705
19. Sunil, Sharma A, Shandil R. Effect of magnetic field dependent viscosity on ferroconvection in the presence of dust particles. J Appl Math Comput. 2008;27:7–22. https://doi.org/10.1007/s12190-008-0055-2
20. Sunil, Divya, Sharma R. The effect of magnetic-field-dependent viscosity on ferroconvection in a porous medium in the presence of dust particles. J Geophys Eng. 2004;1(4):277–286. https://doi.org/10.1088/1742-2132/1/4/006
21. Sharma A, Kumar P et al. Effect of magnetic field dependent viscosity and rotation on ferroconvection in the presence of dust particles. Appl Math Comput. 2006;182(1):82–88. https://doi.org/10.1016/j.amc.2006.03.037
22. Kumar P, Kumar A, Thakur A. Effect of viscosity variation with temperature on convective instability in a hot dusty ferrofluid layer with permeable boundaries. Numer Heat Transf B. 2024;1–18. https://doi.org/10.1080/10407790.2024.2380755
23. Mittal R, Rana U. Effect of dust particles on a layer of micropolar ferromagnetic fluid heated from below saturating a porous medium. Appl Math Comput. 2009;215(7):2591–2607. https://doi.org/10.1016/j.amc.2009.08.063
24. Singh B. Effect of rotation on a layer of micro-polar ferromagnetic dusty fluid heated from below saturating a porous medium. Int J Eng Res Appl. 2016;6(3):4–28.
25. Kumar S, Pundir R, Nadian PK. Effect of dust particles on a rotating

couple-stress ferromagnetic fluid heated from below. Int J Sci Eng Appl Sci. 2020.
26. Nanjundappa C, Pavithra A, Shivakuamara I. Effect of dusty particles on Darcy-Brinkman gravity driven ferro-thermal-convection in a ferrofluid saturated porous layer with internal heat source: influence of boundaries. Int J Appl Comput Math. 2021;7:1–20. https://doi.org/10.1007/s40819-020-00948-6
27. Khan D, Rahman AU, Ali G, Kumam P, Kaewkhao A, Khan I. The effect of wall shear stress on two phase fluctuating flow of dusty fluids by using Lighthill technique. Water. 2021;13(11):1587. https://doi.org/10.3390/w13111587
28. Khan D, Ali G, Kumam P, Rahman AU. A scientific outcome of wall shear stress on dusty viscoelastic fluid along heat absorbing in an inclined channel. Case Stud Therm Eng. 2022;30:101764. https://doi.org/10.1016/j.csite.2022.101764
29. Khan D, Hussien MA, Elsiddieg AM, Lone SA, Hassan AM. Exploration of generalized two phase free convection magnetohydrodynamic flow of dusty tetra-hybrid Casson nanofluid between parallel microplates. Nanotechnol Rev. 2023;12(1):20230102. https://doi.org/10.1515/ntrev-2023-0102
30. Kumam P, Kumam W, Suttiarporn P, Rehman A, et al. Relative magnetic field and slipping effect on Casson dusty fluid of two phase fluctuating flow over inclined parallel plate. S Afr J Chem Eng. 2023;44:135–146. https://doi.org/10.1016/j.sajce.2023.01.010
31. Khan D, Kumam P, Watthayu W, Jarad F. Exploring the potential of heat transfer and entropy generation of generalized dusty tetra hybrid nanofluid in a microchannel. Chin J Phys. 2024;89:1009–1023. https://doi.org/10.1016/j.cjph.2023.10.006
32. Siddheshwar PG. Convective instability of ferromagnetic fluids bounded by fluid-permeable, magnetic boundaries. J Magn Magn Mater. 1995;149(1–2):148–150. https://doi.org/10.1016/0304-8853(95)00358-4
33. Surya D, Gupta A. Thermal instability in a liquid layer with permeable boundaries under the influence of variable gravity. Eur J Mech B Fluids. 2022;91:219–225. https://doi.org/10.1016/j.euromechflu.2021.10.010
34. Chandrasekhar S. Hydrodynamic and hydromagnetic stability. 10th ed. Basingstoke: Courier Corporation; 2013.
35. Prakash J, Kumar R, Kumari K. Thermal convection in a ferromagnetic fluid layer with magnetic field dependent viscosity: A correction applied. Stud Geotech Mech. 2017;39(3):39–46. https://doi.org/10.1515/sgem-2017-0028
36. Beavers GS, Joseph DD. Boundary conditions at a naturally permeable wall. J Fluid Mech. 1967;30(1):197–207. https://doi.org//10.1017/S0022112067001375
37. Kumar P, Thakur A, Kaur M, Kumar A. Numerical investigation of the impact of magnetic field dependent viscosity on darcy–brinkman ferromagnetic convection with permeable boundaries. Special Topics & Reviews in Porous Media: An International Journal. 2025;16(4). https://doi.org/10.1615/SpecialTopicsRevPorousMedia.2024054589

Awneesh Kumar: https://orcid.org/0009-0001-2934-8487
Pankaj Kumar: https://orcid.org/0000-0002-2938-1033
Abhishek Thakur: https://orcid.org/0009-0005-0027-708X
Mandeep Kaur: https://orcid.org/0009-0000-1512-6798